НЕОНАТОЛОГІЯ, ХІРУРГІЯ ТА ПЕРИНАТАЛЬНА МЕДИЦИНА
NEONATOLOGY, SURGERY AND PERINATAL MEDICINE
Т. XV, № 1(55), 2025
VOL. XV, № 1(55), 2025
ISSN 2226-1230 (PRINT) ISSN 2413-4260 (ONLINE)
KEY TITLE: NEONATOLOGÌÂ, HÌRURGÌÂ TA PERINATAL'NA MEDICINA (ONLINE)
ABBREVIATED KEY TITLE: NEONATOL. HÌR. PERINAT. MED. (ONLINE)

UDC: 340.66:616.831-001.31-005.1/.4-005.8
DOI: 10.24061/2413-4260. XV.1.55.2025.19

POLARIZATION REPRODUCTION OF STRUCTURAL ANISOTROPY MAPS OF BRAIN PREPARATIONS FOR DIFFERENTIAL DIAGNOSTICS OF HEMORRHAGES OF TRAUMATIC AND NON-TRAUMATIC GENESIS

***M. Garazdiuk*[1], *O. Ushenko*[2], *O. Dubolazov*[2]**

Bukovinian State Medical University[1],
Yuriy Fedkovych Chernivtsi National University[2]
(Chernivtsi, Ukraine)

Summary

In recent years, modern non-destructive and non-invasive methods of optical diagnostics of biological tissue and fluid preparations have become widely and effectively used in various branches of medicine. Among the wide range of optical methods, one of the most effective has been distinguished – laser polarimetric diagnostics of the polycrystalline structure of biological layers.

The purpose and tasks of the research. *To experimentally test and determine a set of markers for differential diagnosis of the cause of death due to the formation of hemorrhages of traumatic and non-traumatic genesis in the substance of the human brain by using the Muller matrix mapping method with algorithmic reproduction of linear birefringence of native histological brain sections.*

Research materials and methods. *As a research material, native histological sections of human brain taken from the parietal region of head from the deceased, whose cause of death was traumatic hemorrhage – group II (total number n=100), ischemic cerebral infarction – group III (n=100), non-traumatic hemorrhage – group IV (n=100), acute coronary insufficiency – group I – control (n=40), were used. The extracted samples of human brain matter were frozen at a temperature of –70 °C and histological sections were then made using a freezing microtome. Further, the obtained samples were studied using a Stokes polarimeter using the method of azimuthal-invariant experimental measurement of coordinate distributions of the magnitude of the elements of the Muller matrix of native histological sections of the brain from deceased.*

Research results. *In the process of increasing degeneration and necrosis, the level of macrostructural linear birefringence decreases, as well as the transformation of the topographic hierarchy of the polycrystalline architectonics of the brain. As a result, the corresponding random values and their fluctuations in the coordinate distributions of linear birefringence of the structural elements of the polycrystalline architectonics of the experimental brain samples decrease. The topographic structure of algorithmically reproduced maps becomes less homogeneous, small-scale and statistical due to degeneration and necrosis of neural networks. Based on this, prognostic scenarios of changes in the set of digital statistical, correlation, fractal and wavelet markers that determine the pathological transformation of linear birefringence of neural networks of native histological brain sections were substantiated.*

Conclusions. *The diagnostic power of the method of azimuthal-invariant Muller matrix microscopy of native histological sections of the brain of deceased persons due to hemorrhages of traumatic and non-traumatic hegemony has been established at an excellent level (up to 97.5%).*

Key words: *Traumatic Brain Injury; Forensic Medicine; Time of Hemorrhage Formation; Laser Polarimetry, Birefringence; Histological Sections.*

Introduction

In recent years, modern non-destructive and non-invasive methods of optical diagnostics of biological tissues and fluid preparations have been widely and effectively used in various branches of medicine [1,2]. Among a wide range of optical methods, one of the most effective is laser polarimetric diagnostics of the polycrystalline structure of biological layers [3,4]. In particular, the possibility of laser polarimetric high-precision and express differential diagnostics of pathological and necrotic conditions has been demonstrated [4-6]. The methodological generalization and development of laser polarimetry have become the methods and systems of multiparametric Muller matrix polarimetry, which provide comprehensive and complete information about the optically anisotropic component of biological tissues and fluid preparations [2-11].

The most effective at present are applications of such methods in complex tasks of forensic medicine, which are related to determination of the cause and prescription of death, traumatic injuries, etc. [8-11]. It should be noted that the entire arsenal of methods and systems of Muller matrix polarimetry is mainly aimed at determining the criteria and practical application of such markers in differential diagnostics and dynamics of pathological and necrotic changes in tissues and fluids of human organs over short periods of time. At the same time, practically unresearched and currently relevant are issues related to establishing criteria for diagnosing the genesis of hemorrhages in the substance of the human brain.

The aim and tasks of the research: Experimental testing and determination of a set of markers for the differential diagnosis of the cause of death due to the formation of hemorrhages of traumatic and non-traumatic genesis in the substance of the human brain by means of the Muller matrix mapping method with algorithmic reproduction of linear birefringence of native histological brain sections.

Materials and methods. As research material were used native histological sections of human brain matter from the parietal region of the deceased whose cause of death was traumatic hemorrhage – group II (total number n=100), ischemic cerebral infarction – group III (n=100), non-traumatic hemorrhage – group IV (n=100), acute coronary insufficiency – group I – control (n=40). The samples of human brain material, taken during forensic autopsies in the State Medical Establishment «Chernivtsi

Regional Bureau of Forensic Medical Examination», were frozen at –70 °C and then histological sections were made using a freezing microtome.

In the laboratory of the Institute of Physical, Technical and Computer Sciences named after Yuriy Fedkovych, studies of the obtained samples were carried out with the Stokes polarimeter using the method of azimuthal-invariant experimental measurement of coordinate distributions of the size of the elements of the Müller matrix of native histological sections of the brains of deceased persons, which consists of the following set of actions.

1. The brain sample is placed on the mechanical stage of the laser Muller matrix polarimeter (the detailed design and description of the parameters of its optical and optoelectronic elements are given in numerous publications [3-11] and are not given by us).

2. Using a multi-channel polarization filter, four polarization states of the parallel beam of a He-Ne laser with a wavelength of 0.6328 μm irradiating the brain sample are sequentially formed:

- 1st channel – linearly polarized with azimuth 0^0;
- 2nd channel – linearly polarized with azimuth 90^0;
- 3rd channel – linearly polarized with azimuth 45^0;
- 4th channel – right ($\otimes$) circularly polarized.

3. A microlens (magnification ×4) projects an image of the brain sample onto the plane of the photosensitive area of the digital camera, which consists of 1120×960 pixels.

4. A multichannel polarizer-analyzer with six filters is placed in front of the digital camera:

1st filter – linearly polarized with azimuth 0^0;

- 2nd filter – linearly polarized with azimuth 90^0;
- 3rd filter – linearly polarized with azimuth 45^0;
- 4th filter – linearly polarized with azimuth 135^0;
- 5th filter – right ($\otimes$) circularly polarized;
- 6th filter – left ($\otimes$) circularly polarized.

5. The microscopic image of the brain sample passed through each partial polarization filter is discretized by a set of coordinately distributed pixels of the digital camera and enters the interface of the computing device as a two-dimensional digital array.

6. On this basis, for each channel of polarization (0^0; 90^0; 45^0; $\otimes$) irradiation with a parallel laser beam, the four parameters ($St_{i=1;2;3;4}$) of the Stokes vector St are calculated according to the known relations [2-10]:

$$St = \begin{pmatrix} St_1^{0^0;90^0;45^0;\otimes} = R_0^{0^0;90^0;45^0;\otimes} + R_{90}^{0^0;90^0;45^0;\otimes} \\ St_2^{0^0;90^0;45^0;\otimes} = R_0^{0^0;90^0;45^0;\otimes} - R_{90}^{0^0;90^0;45^0;\otimes} \\ St_3^{0^0;90^0;45^0;\otimes} = R_{45}^{0^0;90^0;45^0;\otimes} - R_{135}^{0^0;90^0;45^0;\otimes} \\ St_4^{0^0;90^0;45^0;\otimes} = R_{\otimes}^{0^0;90^0;45^0;\otimes} - R_{\oplus}^{0^0;90^0;45^0;\otimes} \end{pmatrix}. \quad (1)$$

7. Coordinate distributions of the magnitude of partial matrix elements, calculated within the set of all pixels of the photosensitive area of a digital camera, form Muller matrix images (MMI) of optically anisotropic polycrystalline architectonics of brain samples of deceased persons with different genesis of hemorrhage:

$$m_{22} = 0.5(St_2^0 - St_2^{90}); m_{23} = St_2^{45} - m_{21};$$
$$m_{24} = St_2^{\otimes} - m_{21}; m_{31} = 0.5(St_3^0 + St_3^{90});$$
$$m_{32} = 0.5(St_3^0 - St_3^{90}); m_{33} = St_3^{45} - m_{31};$$
$$m_{34} = St_3^{\otimes} - m_{31}; m_{41} = 0.5(St_4^0 + St_4^{90});$$
$$m_{42} = 0.5(St_4^0 - St_4^{90}); m_{43} = St_4^{45} - m_{41};$$
$$m_{44} = St_4^{\otimes} - m_{41}. \quad (2)$$

8. The set of Muller matrix meanings (MMM) is the basis for algorithmic reproduction of linear birefringence (LB) maps of neural networks of the brain:

$$LB = 0{,}5 arcsin\left(\left(m_{24} - m_{42}\right) \Big/ \left(m_{34} - m_{43}\right)\right). \quad (3)$$

The obtained distributions of random values of the quantity LB are algorithmically processed within the following analytical approaches:

Statistical approach in the MATLAB software product calculates central statistical moments of the 1st – 4th orders:

$$Q_1 = \frac{1}{m \times n} \sum_{j=1}^{m \times n} LB_j;$$
$$Q_2 = \sqrt{\frac{1}{m \times n} \sum_{j=1}^{m \times n} (LB^2)_j};$$
$$Q_3 = \frac{1}{Q_2^3} \frac{1}{m \times n} \sum_{j=1}^{m \times n} (LB^3)_j;$$
$$Q_4 = \frac{1}{Q_2^4} \frac{1}{m \times n} \sum_{j=1}^{m \times n} (LB^4)_j, \quad (4)$$

where $Q_{i=1;2;3;4}$ average $St_{i=1}$, dispersion $Q_{i=2}$, asymmetry $Q_{i=3}$ and kurtosis $Q_{i=4}$; $m \times n$ – number of pixels of the digital camera.

The autocorrelation approach provides a description of the correlation homogeneity of coordinate distributions of LB random variables. The main analytical tool of the method is the calculation of two-dimensional and one-dimensional autocorrelation functions (ACF) of LB coordinate distributions in the MATLAB software product.

Each eigenvalue of the ACF characterizes the degree of similarity of the distributions of random values of the quantity LB. Quantitatively, this similarity is characterized by the kurtosis K_4 (the degree of «sharpness» of the ACF peak) and the correlation square SK, which is determined by integration under the calculated correlation function.

Fractal approach. The essence of fractal analysis, which was performed in the MATLAB software product, is to calculate the logarithmic dependences of the power spectral density (PSD) of LB distributions. The fractality

ISSN 2226-1230 (PRINT) ISSN 2413-4260 (ONLINE)

of LB distributions is assessed by the presence and geometric length of linear sections of the slope of the logarithmic dependences of the power spectral density PSD. As an additional quantitative parameter, we chose the «sharpness» of the peak or kurtosis of the power spectral density PSD, which characterizes the distribution by the sizes of the structural elements of LB.

Wavelet approach. Wavelet analysis is generally an analogue of a mathematical microscope for LB distributions of brain preparations of deceased people. In the calculations of the wavelet transformation, the MATLAB program and the «Mexican hat» wavelet function – MHAT with a variable half-width or scale a were used. Such a function is analytically moved (linear movement coordinate b) along the LB distributions. At each point (b) the degree of correlation consistency between LB and the half-width (a) of the wavelet function is determined.

Research Results.

Four groups of representative samples of native histological brain sections of deceased persons were studied on the basis of the following theoretical provisions of multifunctional Müller matrix polarimetry of biological tissue preparations of human organs [2-9]

1. A native histological brain section is a two-component structure consisting of an amorphous (optically isotropic) and an optically anisotropic polycrystalline component.

2. The amorphous component of the brain specimen attenuates the laser radiation due to different absorption coordinates – resulting in a coordinate intensity distribution or a classical microscopic image, which is the subject of traditional histological studies.

3. The polycrystalline architecture of the nervous tissue of the brain is formed by spatially structured networks of neurons and has predominantly linear birefringence.

4. The consequences of traumatization of nervous tissue are manifested in edema and infiltration of neurons. As a result, signs of their degeneration and necrosis increase, which is manifested by a decrease in the level of structural linear birefringence, as well as a transformation of the topographic hierarchy of the polycrystalline architecture of the brain.

5. The most informative method for experimental detection of optically anisotropic architectonics of brain slices is Muller matrix mapping with algorithmic reproduction of linear birefringence maps.

The fragments of Fig. 1 (control group 1), Fig. 3 (group 2), Fig. 5 (group 3) and Fig. 7 (group 4) show a series of algorithmically reproduced coordinate (1) distributions of random values of linear birefringence magnitude and three-dimensional (2) reconstructions of structural anisotropy maps of neuronal networks of experimental samples of native histologic brain The set of Fig. 2 (group 1), Fig. 4 (group 2), Fig. 6 (group 3) and Fig. 8 (group 4) illustrate the results of wavelet (coordinate (1), linear dependences of amplitudes of wavelet coefficients (3)) and fractal (power spectral density PSD (2), logarithmic dependence PSD (4)) algorithmic transformation of LB maps.

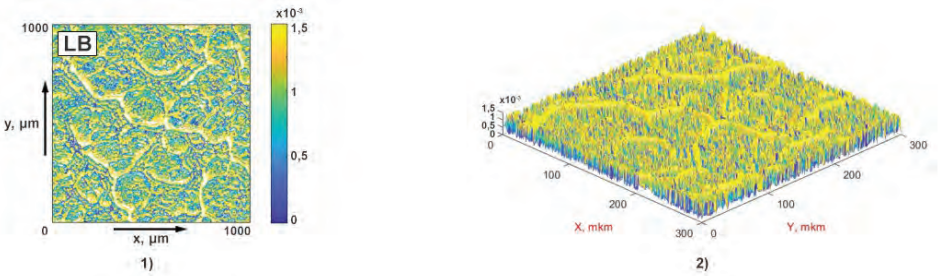

Fig. 1. 2D (fragment (1)) and 3D (fragment (2)) maps of LB neural networks of native histological sections of the deceased brain from control group 1..

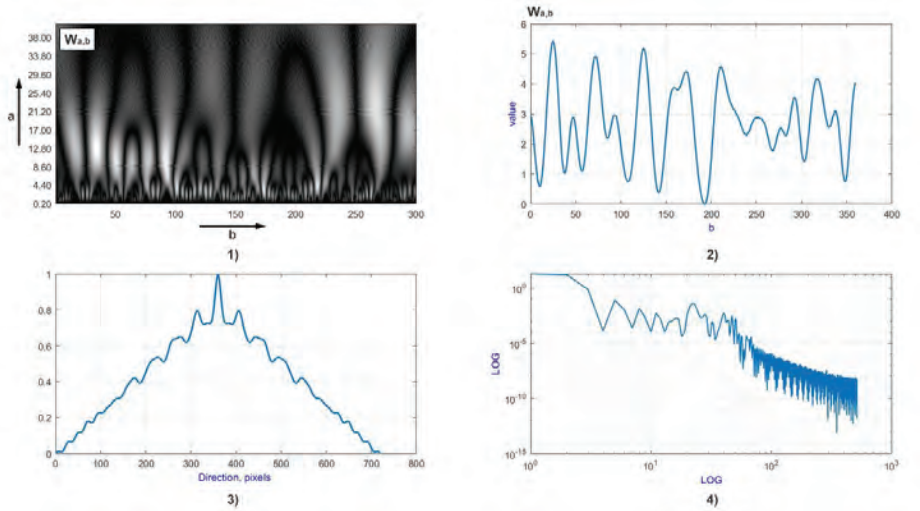

Fig. 2. Coordinate (fragment (1)), linear (fragment (2)), autocorrelation (fragment (3)) and fractal (fragment (4)) characteristics of the wavelet transform of the LB map of a native histological section of the brain of a deceased person from the control group 1.

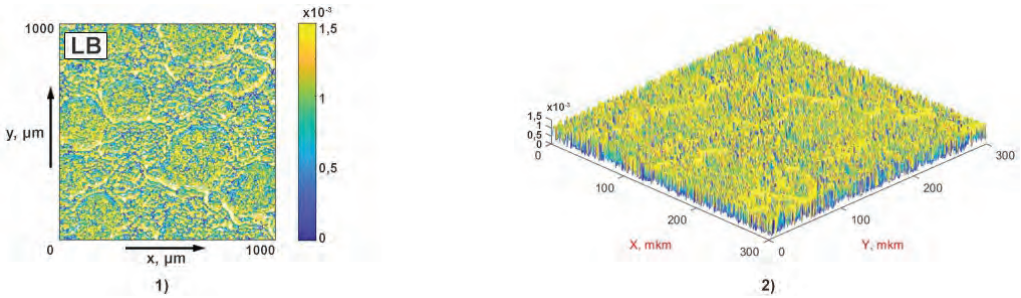

Fig. 3. 2D (fragment (1)) and 3D (fragment (2)) maps of LB neural networks of native histological sections of the deceased brain from group 2.

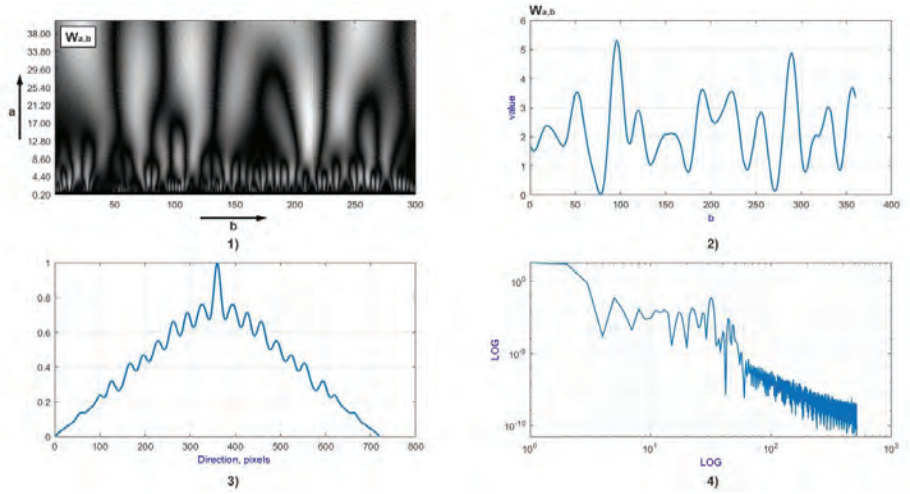

Fig. 4. Coordinate (fragment (1)), linear (fragment (2)), autocorrelation (fragment (3)) and fractal (fragment (4)) characteristics of the wavelet transform of the LB map of a native histological section of the brain of a deceased person from the group 2.

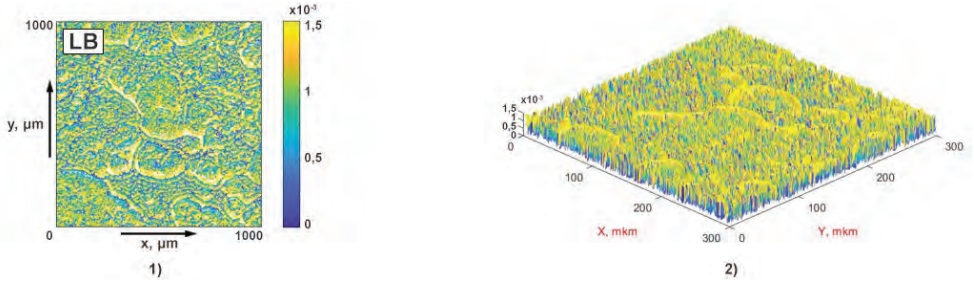

Fig. 5. 2D (fragment (1)) and 3D (fragment (2)) maps of LB neural networks of native histological sections of the deceased brain from group 3.

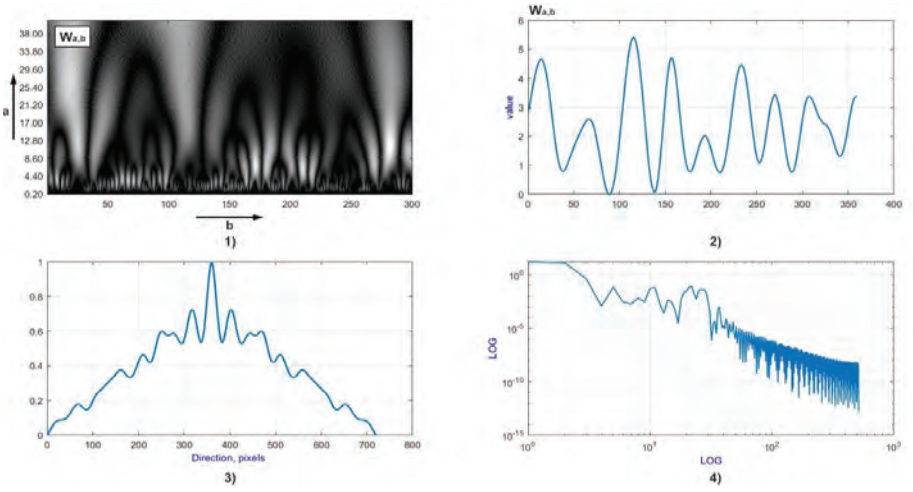

Fig. 6. Coordinate (fragment (1)), linear (fragment (2)), autocorrelation (fragment (3)) and fractal (fragment (4)) characteristics of the wavelet transform of the LB map of a native histological section of the brain of a deceased person from the group 3.

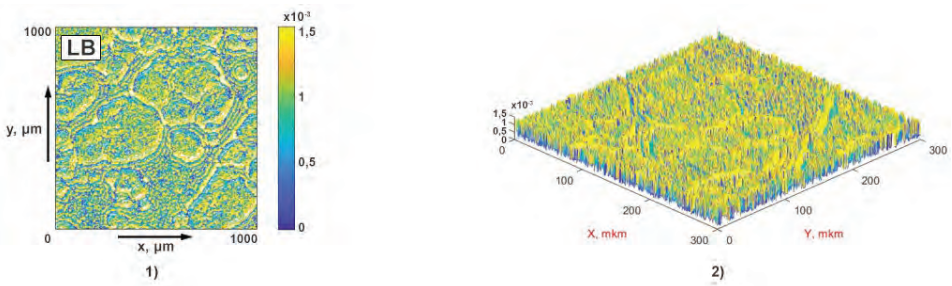

Fig. 7. 2D (fragment (1)) and 3D (fragment (2)) maps of LB neural networks of native histological sections of the deceased brain from group 4.

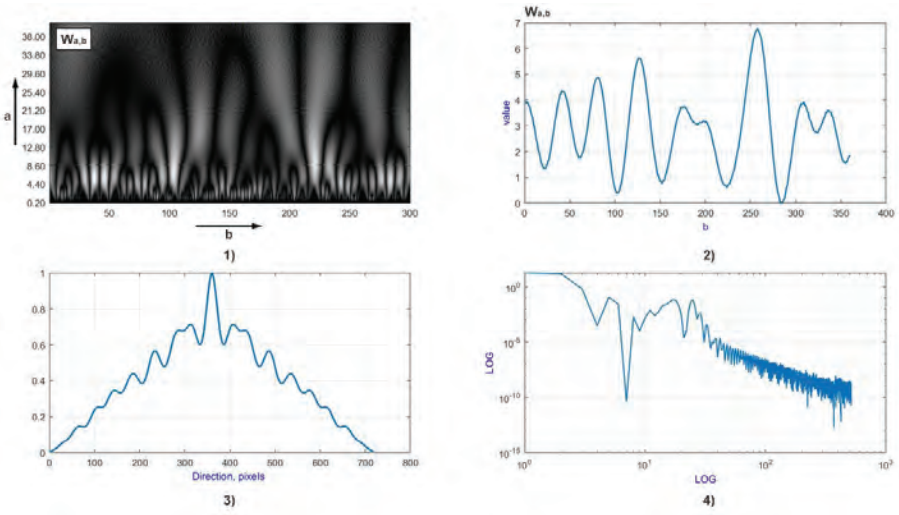

Fig. 8. Coordinate (fragment (1)), linear (fragment (2)), autocorrelation (fragment (3)) and fractal (fragment (4)) characteristics of the wavelet transform of the LB map of a native histological section of the brain of a deceased person from the group 4.

1. For all four groups of brain samples, common patterns were found by comparative analysis of coordinate distributions of the value of the structural anisotropy parameter and data from statistical processing of scale-selective (wavelet), correlation and scale-self-similar (fractal) transformations of polarization-reproduced linear birefringence maps of spatially structured neuronal networks.

2. LB maps of experimental brain samples are coordinate inhomogeneous with random local values of linear birefringence. Quantitatively, this is manifested by different half-widths and peaks of the autocorrelation functions of the amplitude distributions of the wavelet transform coefficients of the ensemble of values of the structural anisotropy parameter.

3. LB maps are formed by large-scale ensembles of local areas (optically anisotropic domains). Quantitatively, this is manifested in different amplitude and period of modulation of wavelet coefficients at different scales of structural optically anisotropic domains of spatially structured neural networks.

4. Fractal analysis of the amplitude distributions of the wavelet transform coefficients of the topographic structure of LB maps revealed the individual number and geometric length of linear sections of the logarithmic dependences of the power spectral density of the distributions of the structural anisotropy parameter within all representative samples of brain samples for different groups of deceased persons.

5. The following pathological transformations of the statistical and topographic structure of the LB maps were observed in different study groups, depending on the cause of death

1) a decrease in the average level and depth of fluctuations of random values of the linear birefringence value, – Fig. 1, Fig. 3, Fig. 5 and Fig. 7 (fragments (1), (2)); 2) an increase in the modulation period of the amplitudes of the wavelet coefficients of the algorithmic scale-selective transformation of the coordinate distributions of the linear birefringence value, – Fig. 2, Fig. 4, Fig. 6 and Fig. 8 (fragments (1), (2)); 3) an increase in the sharpness of the peak of the autocorrelation functions of the distribution of the amplitudes of the wavelet coefficients of the algorithmic transformation of the ensemble of random values of the structural anisotropy value, – Fig. 2, Fig. 4, Fig. 6 and Fig. 8 (fragments (3));

Experimentally revealed patterns can be associated with the proposed model concepts of necrotic changes in the architectonics of brain samples of deceased individuals from experimental groups 2-4.

In the process of increasing degeneration and necrosis, the level of macrostructural linear birefringence decreases, as well as the transformation of the topographic hierarchy of the polycrystalline architectonics of the brain. As a result, the corresponding random values and their fluctuations in the coordinate distributions of LB structural elements of the polycrystalline architectonics of experimental brain samples decrease.

The topographic structure of algorithmically reproduced LB maps becomes less homogeneous, small-scale and statistical due to degeneration and necrosis of neuronal networks. Based on this, the following prognostic scenarios of changes in the set of digital statistical, correlation,

fractal and wavelet markers that determine the pathological transformation of linear birefringence of neuronal networks of native histological brain sections were substantiated:

1) Central statistical moments of the 1st and 2nd order (Q1 mean and Q2 dispersion) – there is a continuous decrease in the average level of linear birefringence due to infiltration and necrotic destruction of neural networks.

2) The central statistical moments of the 3rd and 4th order (asymmetry Q3 and kurtosis Q4) are a sequential increase in quantities that are inversely proportional to the Q1 and Q2 orders.

3) The kurtosis K4 of the autocorrelation functions of the distributions of the amplitudes of the wavelet coefficients increases sequentially, and the corresponding correlation area SK, on the contrary, decreases due to the formation of coordinately inhomogeneous distributions of the parameters of the scale-selective wavelet transform of the LB maps of the necrotically changed neuronal networks of the brain.

4) The asymmetry W3 and kurtosis W4 of the distributions of the amplitudes of the wavelet coefficients increase sequentially due to the increase of the modulation period of the eigenvalues associated with the coordinate inhomogeneity of the linear birefringence maps of the necrotically changed brain architectonics.

Table 1 presents the results of statistical analysis of the results of the azimuthal-invariant Muller matrix polarization reconstruction method of structural anisotropy maps of neural networks of the brain.

Table 1

Statistical markers characterizing linear birefringence maps of neural networks of native histological sections of the brain of deceased

Sample	Native histological brain sections			
$Q_{i=1;2;3;4}$	Group 1	Group 2	Group 3	Group 4
$Q_1 \times 10^{-3}$	1,26±0,065	1,13±0,058	1,09±0,054	1,03±0,047
p_{ik}	$p_1<0,05$; $p_{2;3}<0,05$; $p_{2;4}<0,05$; $p_{3;4}<0,05$			
$Q_2 \times 10^{-3}$	0,34±0,014	0,29±0,013	0,22±0,012	0,16±0,011
p_{ik}	$p_1<0,001$; $p_{2;3}<0,05$; $p_{2;4}<0,05$; $p_{3;4}<0,05$			
Q_3	0,25±0,014	0,34±0,019	0,53±0,025	0,68±0,035
p_{ik}	$p_1<0,001$; $p_{2;3}<0,001$; $p_{2;4}<0,001$; $p_{3;4}<0,001$			
Q_4	0,39±0,022	0,51±0,027	0,65±0,034	0,76±0,039
p_{ik}	$p_1<0,001$; $p_{2;3}<0,001$; $p_{2;4}<0,001$; $p_{3;4}<0,001$			

Digital statistical markers that are most sensitive to necrotic transformation of optically anisotropic brain architecture have been established: asymmetry Q3 of the distribution of random values of the linear birefringence value of neuronal networks of the brain with a diagnostic range of statistically significant change (<0.001) – predicted growth from 0.25 to 0.68; kurtosis Q4 (peak sharpness) of the histogram of the distribution of random values of the parameter of structural anisotropy with a diagnostic range of statistically significant change (<0.001) – predicted growth from 0.39 to 0.76.

On this basis, applying the principles of evidence-based medicine and using statistical markers Q3; Q4, levels of balanced accuracy of the diagnostic power of the method of polarization tomography of linear birefringence were established (see Table 2).

Table 2

Balanced accuracy of statistical markers of differential diagnosis of the genesis of cerebral hemorrhage using the method of Muller matrix microscopy of linear birefringence of neural networks of histological sections of the brain of deceased persons

Sample	Native histological brain sections		
Group	«1-2+4»		
$Q_{i=1;2;3;4}$	Se, %	Sp, %	Ac, %
asymmetry, Q_3	a = 96; b = 4;	c = 94; d = 6;	95
kurtosis, Q_4	a = 97; b = 3;	c = 94; d = 6;	95,5
Group	«2-4»		
$Q_{i=1;2;3;4}$	Se, %	Sp, %	Ac, %
asymmetry, Q_3	a = 95; b = 5;	c = 93; d = 7;	
kurtosis, Q_4	a = 96; b = 4;	c = 94; d = 6;	
Group	«2-3»		
$Q_{i=1;2;3;4}$	Se, %	Sp, %	Ac, %
asymmetry, Q_3	a = 94; b = 6;	c = 92; d = 8;	
kurtosis, Q_4	a = 95; b = 5;	c = 92; d = 8;	
Group	«3-4»		
$Q_{i=1;2;3;4}$	Se, %	Sp, %	Ac, %
asymmetry, Q_3	a = 94; b = 6;	c = 90; d = 10;	
kurtosis, Q_4	a = 94; b = 6;	c = 91; d = 9;	

Where b is the number of false negatives, d is the number of false positives.

The following diagnostic efficiency of statistical differentiation of linear birefringence maps of brain samples with different genesis of hemorrhage has been demonstrated:

Diagnostics («control group 1 – experimental groups 2, 3, 4») – excellent level of balanced accuracy *Ac = 97% – 98%*.

Differentiation (group 2 – group 4) – excellent level of balanced accuracy *Ac = 95% – 98%* .

Differentiation (group 2 – group 3) – very good level of balanced accuracy *Ac = 93% – 94%* .

Differentiation (group 3 – group 4) – good level of balanced accuracy *Ac = 89% – 92%*

Table 3. presents the results of determining additional digital markers for differential diagnostics of the genesis of hemorrhage by statistical, correlation and fractal processing of linear distributions of amplitudes of wavelet transform coefficients of linear birefringence maps of neural networks of native histological sections of the brains of deceased individuals.

Table 3

Correlation and fractal markers characterizing wavelet transform of linear birefringence maps of neural networks of native histological sections of deceased brains

Sample	Native histological brain sections			
Groups	Group 1	Group 2	Group 3	Group 4
Parameters	Wavelet			
asymmetry, W_3	0,081±0,004	0,12±0,007	0,21±0,012	0,33±0,017
p_{ik}	p_1<0,001; $p_{2;3}$<0,001; $p_{2;4}$<0,05; $p_{3;4}$<0,001			
kurtosis, W_4	0,91±0,045	1,34±0,076	1,96±0,11	2,79±0,15
p_{ik}	p_1<0,001; $p_{2;3}$<0,001; $p_{2;4}$<0,05; $p_{3;4}$<0,001			
Parameters	Autocorrelation			
kurtosis, K_4	1,11±0,053	0,92±0,054	0,74±0,039	0,41±0,021
p_{ik}	p_1<0,001; $p_{2;3}$<0,001; $p_{2;4}$<0,05; $p_{3;4}$<0,001			
Square, SK	0,191±0,001	0,222±0,011	0,246±0,001	0,281±0,0011
p_{ik}	p_1<0,001; $p_{2;3}$<0,001; $p_{2;4}$<0,05; $p_{3;4}$<0,001			

Analysis of the results of the algorithmic diagnostic correlation and fractal processing of the distributions of the amplitudes of the wavelet transform coefficients of the LB maps revealed the following digital diagnostic markers: correlation kurtosis K4, the value of which characterizes the sharpness of the peak of the autocorrelation functions of the distributions of the amplitudes of the wavelet transform coefficients of the structural anisotropy maps of neuronal networks of native histological brain sections of deceased persons with a diagnostic range of statistically significant change (<0.001) – predicted decrease from 1.11 to 0.41; correlation square SK of the autocorrelation function of the linear distribution of the amplitudes of the wavelet coefficients with a diagnostic range of statistically significant change (<0.001) – predicted increase from 0.191 to 0.281;

Asymmetry of distributions of wavelet amplitude values of linear birefringence map coefficients of neural networks of experimental brain samples of deceased persons W3 with diagnostic range of statistically significant change (<0.001) – predicted increase from 0.081 to 0.33; kurtosis W4 of distributions of wavelet amplitude values of LB map coefficients of neural networks with diagnostic range of statistically significant change (<0.001) – predicted increase from 0.91 to 2.79.

Table 4 shows the results of determining the operational characteristics (sensitivity, specificity and balanced accuracy) of the diagnostic power of the method of azimuthal-invariant mapping of LB maps of native histological brain sections of deceased persons using the identified digital statistical and correlation markers of wavelet parameters.

Table 4

Balanced accuracy of correlation and fractal markers for differential diagnosis of hemorrhage genesis by polarization reconstruction of LB neural network maps of native histological brain sections of deceased individuals

Sample	Native histological brain sections		
Groups	«1-2+4»		
$Q_{i=1;2;3;4}$	Se, %	Sp, %	Ac, %
asymmetry, W_3	a = 98; b = 2;	c = 96; d = 4;	97
kurtosis, W_4	a = 98; b = 2;	c = 97; d = 3;	97,5
kurtosis, K_4	a = 99; b = 1;	c = 95; d = 5;	97
Square ACF, SK	a = 98; b = 2;	c = 96; d = 4;	95

Continuation of the table 4

Sample	Native histological brain sections		
Groups	«2-4»		
$Q_{i=1;2;3;4}$	Se, %	Sp, %	Ac, %
asymmetry, W_3	a = 98; b = 2;	c = 95; d = 5;	96,5
kurtosis, W_4	a = 98; b = 2;	c = 96; d = 4;	97
kurtosis, K_4	a = 98; b = 2;	c = 95; d = 5;	96,5
Square ACF, SK	a = 97; b = 3;	c = 94; d = 6;	95,5
Groups	«2-3»		
$Q_{i=1;2;3;4}$	Se, %	Sp, %	Ac, %
asymmetry, W_3	a = 97; b = 3;	c = 95; d = 5;	96
kurtosis, W_4	a = 98; b = 2;	c = 95; d = 5;	96,5
kurtosis, K_4	a = 97; b = 3;	c = 94; d = 6;	95,5
Square ACF, SK	a = 96; b = 4;	c = 92; d = 8;	94
Groups	«3-4»		
$Q_{i=1;2;3;4}$	Se, %	Sp, %	Ac, %
asymmetry, W_3	a = 96; b = 4;	c = 94; d = 6;	95
kurtosis, W_4	a = 97; b = 3;	c = 95; d = 5;	96
kurtosis, K_4	a = 96; b = 4;	c = 95; d = 5;	95,5
Square ACF, SK	a = 95; b = 5;	c = 92; d = 8;	93,5

The following levels of diagnostic differentiation accuracy were determined for:

Correlation markers K_4; SK wavelet transform of polarization reconstructed LB maps:

Diagnostics («control group 1 – experimental groups 2, 3, 4») – excellent level of balanced accuracy *Ac = 95% – 97%* .

Differentiation (group 2 – group 4) – excellent level of balanced accuracy *Ac = 95,5% – 96,5%*.

Differentiation (group 2 – group 3)– very good (*SK*) *Ac = 93,5%* and excellent level (K_4) *Ac = 95,5%* of balanced accuracy.

Differentiation (group 3 – group 4)– very good (*SK*) *Ac = 93,5%* and excellent level (K_4) *Ac = 95,5%* of balanced accuracy.

2. Statistical markers of the amplitude distributions of wavelet transform coefficients W_3, W_4:

Diagnostics («control group 1 – experimental groups 2, 3, 4») – excellent level *Ac = 97% – 97,5%* of balanced accuracy.

Differentiation (group 2 – group 4)– excellent level of balanced accuracy *Ac = 96,5% – 97%*.

Differentiation (group 2 – group 3) – excellent level *Ac = 96% – 96,5%* of balanced accuracy.

Differentiation (group 3 – group 4)– very good (W_3) *Ac = 95%* and excellent level (W_4) *Ac = 96%* of balanced accuracy.

Conclusions

1. The method of azimuthally invariant Muller matrix microscopy with algorithmic reproduction of linear birefringence maps of polycrystalline architectonics of neuronal networks of experimental samples of native histological sections of brains of deceased persons with traumatic and non-traumatic cerebral hemorrhage has been experimentally tested.

2. Within the framework of a comprehensive statistical analysis of the correlation and wavelet transformation of coordinate distributions of random values of the magnitude of linear birefringence, a set of digital markers (central statistical moments of the 3rd and 4th orders of the distributions of the anisotropy parameter and the amplitudes of the wavelet transform coefficients, as well as kurtosis and correlation area of autocorrelation functions of such distributions) for differential diagnostics of necrotic changes in structural anisotropy of native histological sections of brains of deceased persons were determined, and the values of balanced accuracy of differential diagnostics of traumatic and non-traumatic genesis of hemorrhages were established.

3. The diagnostic power of the method of azimuthal-invariant Muller matrix microscopy with algorithmic reproduction of linear birefringence maps of neuronal networks of native histological sections of the brain of deceased persons due to traumatic and non-traumatic hemorrhages was established at an excellent level (up to 97,5%).

Prospects for further research. In order to increase the sensitivity and accuracy of differential diagnostics of the genesis of cerebral hemorrhage, the possibilities of testing the above-mentioned method of Muller matrix mapping of native histological brain sections with algorithmic reproduction of maps of another mechanism of optical anisotropy – circular birefringence, associated with the optical activity of individual molecular complexes, are being investigated.

Conflict of interest: none.

Source of funding: The study was carried out with the support of a grant from the National Research Foundation of Ukraine № 2023.03/0174.

ISSN 2226-1230 (PRINT) ISSN 2413-4260 (ONLINE)

References:

1. Bertozzi G, Maglietta F, Sessa F, Scoto E, Cipolloni L, Di Mizio G, et al. Traumatic Brain Injury: A Forensic Approach: A Literature Review. Curr Neuropharmacol. 2020;18(6):538-50. DOI: http://doi.org/10.2174/1570159x17666191101123145 PMID: 31686630; PMCID: PMC7457403.
2. Ghosh N, Vitkin IA. Tissue polarimetry: concepts, challenges, applications, and outlook. J Biomed Opt. 2011;16(11):110801. DOI: http://doi.org/10.1117/1.3652896 PMID: 22112102.
3. Layden D, Ghosh N, Vitkin A. Quantitative Polarimetry for Tissue Characterization and Diagnosis. In: Wang RK, Tuchin VV, editors. Advanced Biophotonics. CRC Press; 2013. Chapter 13, p. 73-108. DOI: http://doi.org/ 10.1201/b15256-3
4. Vitkin A, Ghosh N, de Martino A. Tissue Polarimetry. In: Andrews DL, editor. Photonics: Scientific Foundations, Technology and Applications. John Wiley & Sons, Ltd; 2015. Chapter 7, p. 239-321. DOI: https://doi.org/10.1002/9781119011804.ch7
5. Angelsky OV, Ushenko AG, Mokhun II, Zenkova CY, Bogatyryova HV, Felde CV. al. Optical Measurements: Polarization and Coherence of Light Fields. In: Cocco L, editor. Modern Metrology Concerns. InTech; 2012. Chapter 10, 56 p. DOI: http://doi.org/10.5772/36553
6. Ushenko AG, Dubolazov OV, Ushenko VA, Novakovskaya OY, Olar OV. Fourier polarimetry of human skin in the tasks of differentiation of benign and malignant formations. Appl Opt. 2016;55(12): B56-60. DOI: http://doi.org/10.1364/AO.55.000B56 PMID: 27140132.
7. Hu Z, Bachinsky VT, Vanchulyak OY, Soltys IV, Ushenko YA, Ushenko AG, et al. Spectral Phase Measurement of Laser Images of Sections of Biological Tissues of a Human Corpse for Death Time Detection. In: Phase Mapping of Human Biological Tissues. Springer Briefs in Applied Sciences and Technology; 2023. Part F697, p. 53-70. DOI: http://doi.org/10.1007/978-981-99-3269-6_4
8. Ushenko YA, Bachinsky VT, Bezhenar IL, Vanchulyak OY, Litvinenko OY, Soltys IV, et al. Determination of the Lifetime and Post-mortal Nature and Temporal Dynamics of the Formation of Skin Abrasions. In: Laser Polarimetry of Biological Tissues. Springer Briefs in Applied Sciences and Technology; 2023. p. 27-42. DOI: https://doi.org/10.1007/978-981-99-1734-1_3
9. Hu Z, Ushenko YA, Litvinenko OY, Gorsky MP, Vanchulyak OY, Mikirin I, et al. Materials and Methods of Research in Laser Polarimetry Data Processing of Biological Tissues for Forensic Determining the Age of Injury In: Laser Polarimetry of Biological Tissues. Springer Briefs in Applied Sciences and Technology; 2023. p. 9-26. DOI: http://doi.org/10.1007/978-981-99-1734-1_2
10. Hu Z, Bachinsky VT, Vanchulyak OY, Soltys IV, Ushenko YA, Ushenko AG, et al. Novel Diagnosis Capabilities and Prospects for Determining Post-mortem Changes in Biological Tissues and the Time of Hematoma Formation in Forensic Medicine. In: Phase Mapping of Human Biological Tissues. Springer Briefs in Applied Sciences and Technology; 2023. SpringerBriefs in Applied Sciences and Technology: 2023. p. 1-10. DOI: https://doi.org/10.1007/978-981-99-3269-6_1
11. Ushenko YA, Hu Z, Soltys IV, Dubolazov OV, Olar OV, Gordey I, et al. Study of Two-Dimensional Polarization Maps of the Skin for Differentiation of Lifetime and Postmortal Nature and Temporal Dynamics of Abrasions. In: Laser Polarimetry of Biological Tissues. Springer Briefs in Applied Sciences and Technology; 2023. p. 43-75. DOI: http://doi.org/10.1007/978-981-99-1734-1_4

ПОЛЯРИЗАЦІЙНЕ ВІДТВОРЕННЯ МАП СТРУКТУРНОЇ АНІЗОТРОПІЇ ПРЕПАРАТІВ ГОЛОВНОГО МОЗКУ ДЛЯ ДИФЕРЕНЦІАЛЬНОЇ ДІАГНОСТИКИ КРОВОВИЛИВІВ ТРАВМАТИЧНОГО ТА НЕТРАВМАТИЧНОГО ҐЕНЕЗУ

***М. С. Гараздюк*[1], *О. Г. Ушенко*[2], *О. В. Дуболазов*[2]**

Буковинський державний медичний університет[1],
Чернівецький національний університет імені Юрія Федьковича[2]
(Чернівці, Україна)

Резюме.

За останні роки у різноманітних галузях медицини широкого та ефективного розповсюдження набули сучасні неруйнівні та неінвазивні методи оптичної діагностики препаратів біологічних тканин і рідин. Серед широкого спектру оптичних методів виокремився один з найбільш ефективних – лазерна поляриметрична діагностика полікристалічної структури біологічних шарів.

Мета і завдання дослідження: експериментально апробувати і визначити сукупність маркерів диференціальної діагностики причини смерті внаслідок утворення крововиливів травматичного та нетравматичного ґенезу в речовину головного мозку людини шляхом використання методу Мюллер-матричного картографування з алгоритмічним відтворенням лінійного двопроменезаломлення нативних гістологічних зрізів мозку.

Матеріали та методи дослідження. У якості дослідного матеріалу використовувалися нативні гістологічні зрізи речовини головного мозку людини з тім'яної ділянки від померлих, причиною смерті яких були крововиливи травматичного ґенезу – II група (загальна кількість n=100), інфаркт мозку ішемічного генезу – III група (n=100), крововилив нетравматичного ґенезу – IV група (n=100), гостра коронарна недостатність – I група – контроль (n=40). Вилучені зразки речовини головного мозку людини заморожували при температурі –70 °С та надалі виготовлялися гістологічні зрізи за допомогою заморожуючого мікротома. Надалі були проведені дослідження отриманих зразків за допомогою Стокс-поляриметра методом азимутально-інваріантного експериментального вимірювання координатних розподілів величини елементів матриці Мюллера нативних гістологічних зрізів мозку померлих.

Результати дослідження. У процесі наростання дегенерації та некрозу знижується рівень макроструктурного лінійного двопроменезаломлення, а також трансформації топографічної ієрархії полікристалічної архітектоніки мозку. У результаті зменшуються відповідні випадкові значення і їх флуктуації у координатних розподілах лінійного двопроменезаломлення структурних елементів полікристалічної архітектоніки дослідних зразків мозку. Топографічна структура алгоритмічно відтворених мап стає менш однорідною, дрібномасштабною та статистичною за рахунок дегенерації та некрозу нейронних сіток. Виходячи з цього було обґрунтовано прогностичні сценарії зміни сукупності цифрових статистичних, кореляційних, фрактальних і вейвлет маркерів, які визначають патологічну трансформацію лінійного двопроменезаломлення нейронних мереж нативних гістологічних зрізів мозку.

Висновки. Установлено діагностичну силу методу азимутально-інваріантної Мюллер-матричної мікроскопії нативних гістологічних зрізів мозку померлих внаслідок крововиливів травматичного та нетравматичного ґегезу на відмінному рівні (до 97,5%).

Ключові слова: черепно-мозкова травма; судова медицина; час утворення крововиливу; лазерна поляриметрія, двопроменезаломлення; гістологічні зрізи.

Contact information:
M. Garazdiuk – PhD, Associate Professor of Department of Forensic Medicine and Medical Law of Bukovinian State Medical University (Chernivtsi, Ukraine)
e-mail: m.garazdiuk@gmail.com
ORCID: http://orcid.org/0000-0002-7811-3211
ResearcherID: http://www.researcherid.com/rid/C-8134-2017

O. Ushenko. – Doctor of Physical and Mathematical Sciences, Professor, Full Member of the Academy of Engineering Sciences of Ukraine; Academician of the Academy of Sciences of Higher Education of Ukraine, Head of the Department of Optics and Publishing and Printing of Yuriy Fedkovych Chernivtsi National University (Chernivtsi, Ukraine)
e-mail: o.ushenko@chnu.edu.ua
ORCID: http://orcid.org/0009-0002-5088-592X

O. Dubolazov – Doctor of Physical and Mathematical Sciences, Professor, Professor of the Department of Optics and Publishing and Printing of Yuriy Fedkovych Chernivtsi National University (Chernivtsi, Ukraine)
e-mail: a.dubolazov@chnu.edu.ua
ORCID: http://orcid.org/0000-0003-1051-2811
Scopus Author ID: https://www.scopus.com/authid/detail.uri?authorId=35318204300

Контактна інформація:
Гараздюк М. С. – к.мед.н., доцент кафедри судової медицини та медичного правознавства Буковинського державного медичного університету (м.Чернівці, Україна)
e-mail: m.garazdiuk@gmail.com
ORCID: http://orcid.org/0000-0002-7811-3211
ResearcherID: http://www.researcherid.com/rid/C-8134-2017

Ушенко О. Г. – д фіз.-мат.н., професор, Дійсний член Академії інженерних наук України; Академік Академії наук вищої школи України, завідувач кафедри оптики і видавничо-поліграфічної справи Чернівецького національного університету імені Юрія Федьковича (м. Чернівці, Україна)
e-mail: o.ushenko@chnu.edu.ua
ORCID: http://orcid.org/0009-0002-5088-592X

Дуболазов О. В. – д.фіз.-мат.н., професор, професор кафедри оптики і видавничо-поліграфічної справи Чернівецького національного університету імені Юрія Федьковича (м. Чернівці, Україна)
e-mail: a.dubolazov@chnu.edu.ua
ORCID: http://orcid.org/0000-0003-1051-2811
Scopus Author ID: https://www.scopus.com/authid/detail.uri?authorId=35318204300

Received for editorial office on 17/01/2025
Signed for printing on 20/03/2025